

Two distinct inputs to an avian song nucleus activate different glutamate receptor subtypes on individual neurons

(*N*-methyl-D-aspartate/excitatory postsynaptic potentials/birdsong)

RICHARD MOONEY AND MASAKAZU KONISHI

Division of Biology 216-76, California Institute of Technology, Pasadena, CA 91125

Contributed by Masakazu Konishi, January 23, 1991

ABSTRACT Although neural circuits mediating various simple behaviors have been delineated, those generating more complex behaviors are less well described. The discrete structure of avian song control nuclei promises that circuits controlling complex behaviors, such as birdsong, can also be understood. To this end, we developed an *in vitro* brain slice preparation containing the robust nucleus of the archistriatum (RA), a forebrain song control nucleus, and its inputs from two other song nuclei, the caudal nucleus of the ventral hyperstriatum (Hvc) and the lateral part of the magnocellular nucleus of the anterior neostriatum (L-MAN). Using intracellular recordings, we examined the pharmacological properties of the synapses made on RA neurons by L-MAN and Hvc axons. Electrical stimulation of the L-MAN and the Hvc fiber tracts evoked excitatory postsynaptic potentials (EPSPs) from >70% of RA neurons when slices were prepared from male birds of 40–90 days of age, suggesting that many individual RA neurons receive excitatory input from L-MAN and Hvc axons. The “L-MAN” EPSPs were blocked by the *N*-methyl-D-aspartate (NMDA) receptor antagonist D-(–)-2-amino-5-phosphonovaleric acid (D-APV) as well as the broad-spectrum glutamate receptor antagonist kynurenic acid but were relatively unaffected by the non-NMDA receptor blocker 6-cyano-7-nitroquinoxaline-2,3-dione (CNQX). In contrast, “Hvc” EPSPs were relatively insensitive to D-APV but almost completely abolished by CNQX. These experiments suggest that L-MAN and Hvc axons provide pharmacologically distinct types of excitatory input to many of the same RA neurons.

The differential activation of *N*-methyl-D-aspartate (NMDA) and non-NMDA glutamate receptors can produce pronounced differences in the output patterns of certain neural circuits (1–3). We report here that two distinct inputs to the same neuron activate primarily NMDA or non-NMDA receptors in the robust nucleus of the archistriatum (RA), which is one of the brain areas that controls song in birds. The neural signals for song descend from the caudal part of the nucleus of the ventral hyperstriatum (Hvc) to the RA and from there to the tracheosyringeal portion of the hypoglossal nucleus (nXIIIts), which in turn innervates the vocal muscles used in singing (4–6). This chain of nuclei thus constitutes the motor pathway for song. The Hvc is linked to the RA by another series of nuclei, which includes area X, the medial part of the dorsolateral thalamus, and the lateral part of the magnocellular nucleus of the anterior neostriatum (L-MAN) (7, 8). This pathway presumably carries auditory information necessary for the control of song development (9–11). The RA is thus located at the point of convergence between the vocal motor and auditory pathways. The colocalization of two distinct glutamate receptor subtypes at such a location

might have special significance for the well-known vocal plasticity exhibited by songbirds.

MATERIALS AND METHODS

Brain slices were prepared from 40- to 90-day-old male zebra finches (*Taeniopygia guttata*) or Bengalese finches (*Lonchura striata*) obtained from our breeding colony (all dates refer to posthatch age: the hatch day is posthatch 0). Birds were anesthetized with ketamine hydrochloride (0.03–0.06 ml), followed by 5–10 min of Metofane (Pitman–Moore, Washington Crossing, NJ) inhalation, which was discontinued when the respiratory rate decreased markedly. After a second, larger injection of ketamine (0.06–0.09 ml), the bird was decapitated. The brain was removed and placed in ice-cold artificial cerebrospinal fluid (ACSF; see below for recipes) that had been equilibrated with 95% O₂/5% CO₂. The brain was blocked transversely about 5 mm rostral of the bifurcation of the midsagittal sinus, and the caudal half of the brain was glued (Loctite, Cleveland) rostral face down to the stainless steel tray of the vibratome. Coronal slices were cut at 400 μm thickness and transferred to an interface-type chamber. The ACSF in the interface chamber was supplemented with 0.1% bovine serum albumin (Sigma) and DL-(–)-2-amino-5-phosphonovaleric acid (DL-APV) to a final concentration of 100 μM. The upper surface of the slice was exposed to a humidified atmosphere of 95% O₂/5% CO₂.

After a 1- to 2-hr recovery period, individual brain slices were transferred to a semisubmersion type recording chamber maintained at 35°C, with a perfusion rate of 3–5 ml/min. The fluid level was lowered to within <500 μm of the upper surface of the slice. ACSF was warmed to 35°C and gassed with 95% O₂/5% CO₂ before entering the chamber. Humidified 95% O₂/5% CO₂ was also supplied to the recording chamber.

Anatomical reconstruction has shown that L-MAN and Hvc axons describe different paths to reach RA (personal observations; see also ref. 8). Although L-MAN and Hvc fibers travel in roughly parallel dorsoventral trajectories toward RA, L-MAN fibers are displaced laterally to those arising from Hvc. Ultimately, L-MAN axons turn and enter RA along its lateral face, whereas Hvc axons, being more medially situated, enter RA along its dorsal edge (see Fig. 1). Therefore, coronal slices containing RA were prepared that allowed the L-MAN and Hvc fiber tracts to be electrically stimulated independently of one another. Bipolar tungsten stimulating electrodes were placed ≤1.0 mm lateral and dorsal to nucleus RA, in areas containing the L-MAN or Hvc axon tracts entering the nucleus (see Fig. 1). Electrical

Abbreviations: NMDA, *N*-methyl-D-aspartate; EPSP, excitatory postsynaptic potential; RA, robust nucleus of the archistriatum; Hvc, caudal nucleus of the ventral hyperstriatum; L-MAN, lateral part of the magnocellular nucleus of the anterior neostriatum; CNQX, 6-cyano-7-nitroquinoxaline-2,3-dione; ACSF, artificial cerebrospinal fluid; APV, 2-amino-5-phosphonovaleric acid.

The publication costs of this article were defrayed in part by page charge payment. This article must therefore be hereby marked “advertisement” in accordance with 18 U.S.C. §1734 solely to indicate this fact.

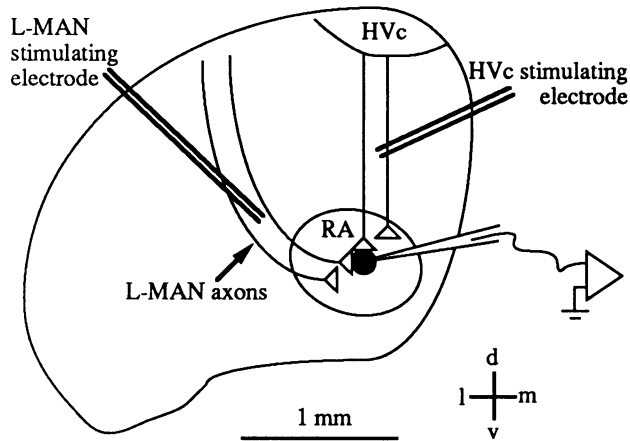


FIG. 1. A schematic of the *in vitro* finch forebrain slice preparation shows the placement of the intracellular recording electrode in a RA neuron and the location of the extracellular, bipolar stimulating electrodes in the L-MAN (lateral) and HVC (dorsal) fiber tracts entering RA.

stimulation of each fiber tract was accomplished by applying brief voltages (0.5–20 V), 100 μ sec in duration, at a frequency of 0.1–1 Hz [WPI (New Haven, CT) Pulsemaster], to the stimulating electrodes.

Drugs were delivered to the slice by switching between various bathing solutions by means of a solenoid-operated valve assembly (General Valve, Fairfield, NJ). Alternatively, a pressure-driven puffer pipette (WPI PicoPump), prepared from 1-mm capillary glass and drawn to a final tip diameter of 20–50 μ m, was positioned within 400 μ m of the recording site. Drugs of choice were dissolved in ACSF at known concentrations and then loaded into the pipette. With this method, drug concentrations refer to the pipette solution. The actual bath concentrations were assumed to be substantially lower than the upper limit set by the pipette concentration. D-APV and 6-cyano-7-nitroquinoxaline-2,3-dione (CNQX) were purchased from Tocris Neuramin (Essex, England). All other drugs were purchased from Sigma.

RA neurons were impaled with 50- to 150-M Ω electrodes fabricated on a Brown-Flaming microelectrode puller from 1-mm borosilicate glass (WPI 1B1001F) and filled with 3 M potassium acetate. The postsynaptic membrane potential was amplified [NeuroData (New York) IR-283 intracellular amplifier, bridge circuit] and individual events were stored on videotape in a pulse code format (NeuroData Neuro-Corder DR-484). Signals were low pass filtered at 5 kHz, digitized at 10 kHz, signal averaged, and analyzed with the aid of digital oscilloscope software written by Larry Proctor (California Institute of Technology) for a Masscomp (Westford, MA) graphics workstation. Synaptic potentials are the averages of 6–16 individual traces. Measurements of the excitatory postsynaptic potential (EPSP) slope were calculated over the first millisecond of the EPSP, starting from the EPSP onset. EPSP amplitudes were calculated as the maximum positive deflection from baseline. Quantification of the EPSP amplitude reflects the mean, as normalized to the control value preceding drug treatment, \pm SEM. Average values of an EPSP's peak latency and onset slope were not normalized. Statistical significance was determined by an unpaired *t* test (two-tailed). Resting potential was calculated as the difference between the observed potential immediately before and after withdrawal of the recording electrode from the cell. In some cases, dc hyperpolarization of the postsynaptic cell membrane was used to suppress spontaneously occurring action potentials.

The ACSF recipe is as follows (all concentrations are mM): NaCl, 134.0; NaHCO₃, 25.7; NaH₂PO₄, 1.3; KCl, 3.0; MgSO₄ (7H₂O), 1.3; CaCl₂(2H₂O), 2.4; glucose, 12.0; urea, 1.0. For

high divalent ACSF, CaCl₂(2H₂O) and MgSO₄(7H₂O) were 4.0 mM each. For very high divalent ACSF, CaCl₂(2H₂O) and MgSO₄(7H₂O) were 8 mM each.

RESULTS

The majority of RA neurons responded to L-MAN and HVC fiber stimulation (72 of 98 cells in 30 experiments). Electrical stimulation in the L-MAN and HVC fiber tracts could evoke depolarizing potentials from such "dually innervated" RA neurons (two lower amplitude traces in Fig. 2). Since the depolarizing potentials evoked by stimulating either input by itself could exceed spike threshold, they were classified as excitatory (EPSPs). The "L-MAN" and "HVC" EPSPs recorded from 25 dually innervated RA neurons were analyzed in greater detail.

A consistent feature of the subthreshold L-MAN and HVC EPSPs was that their shapes differed from each other, as shown in Fig. 2. L-MAN EPSPs displayed a shallower onset slope and took relatively longer to reach peak amplitude, whereas HVC EPSPs exhibited a steeper onset slope and a substantially shorter time to peak. In 25 dually innervated RA neurons, the L-MAN EPSP onset slope averaged 1.06 ± 0.13 mV/msec, significantly less than the value of 1.57 ± 0.14 mV/msec obtained for the HVC EPSP ($P < 0.009$, $n = 25$). In the same RA neurons, the time to peak of the L-MAN response, at 12.28 ± 0.89 msec, was significantly longer than the value of 7.12 ± 0.76 msec measured for the HVC EPSP ($P < 0.0001$, $n = 25$). L-MAN EPSPs were characterized by a slower initial time course than those evoked by HVC fiber stimulation.

The interactions between the L-MAN and HVC EPSPs were examined by stimulating the two fiber pathways simultaneously. Since simultaneous stimulation of the L-MAN and HVC fiber pathways often drove the cell past spike threshold, the individual stimulus intensities were reduced until the simultaneous stimulation of the two inputs did not evoke an action potential. The *linear sum* of the L-MAN and HVC EPSPs, computed by digitally adding the EPSPs evoked by stimulating either input alone, was compared to the EPSP

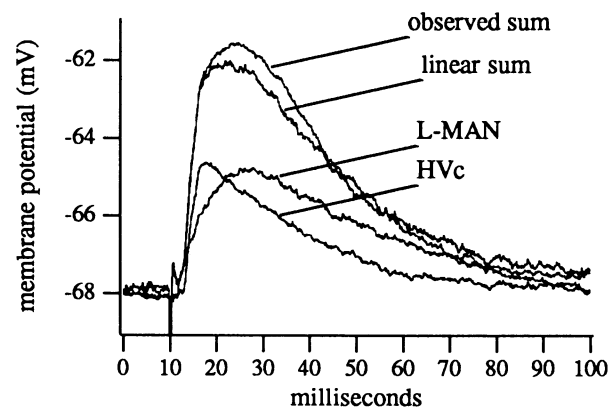


FIG. 2. Electrical stimulation of the L-MAN and HVC fiber tracts evoked EPSPs from the majority of RA neurons from which we recorded. The EPSPs shown here, recorded *in vitro* from a typical dually innervated RA neuron, were obtained in a brain slice prepared from a 50-day-old male finch. The L-MAN EPSP exhibited a consistently shallower onset slope and longer time to peak than did the HVC EPSP. The L-MAN and HVC EPSPs summed in a nearly linear fashion when the two fiber tracts were stimulated simultaneously. The actual EPSP observed when driving the two inputs together (*observed sum*) slightly exceeded the *linear sum* of the two EPSPs obtained when driving each input separately. The cell is shown at its actual resting potential, recorded in high divalent ACSF. In all cases, electrical stimuli were applied at $t = 10$ msec.

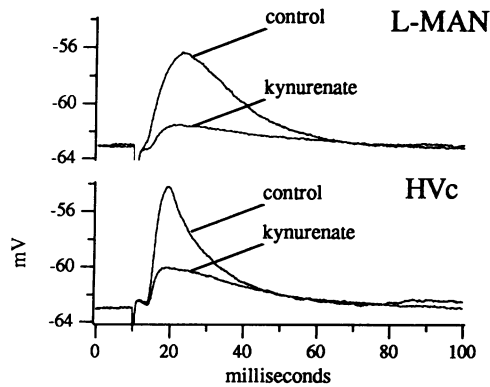


FIG. 3. Kynurenic acid (10 mM applied from a puffer pipette) substantially reduced the L-MAN and the HVC EPSPs recorded from dually innervated RA neurons. The cell is shown at its actual resting potential. Recordings were made in high divalent ACSF; the brain slice was prepared from a 70-day-old male finch. Stimuli were applied to the L-MAN or HVC fiber tracts at $t = 10$ msec.

evoked by stimulating the two inputs simultaneously (*observed sum*). The results of such a comparison can be seen in Fig. 2. In six cases analyzed in this manner, the observed sum closely approximated the linear sum, although in five of these cases, the observed sum actually exceeded the linear sum of the L-MAN and HVC EPSPs by a slight amount.

The pharmacological nature of the L-MAN and HVC EPSPs was investigated by applying specific neurotransmitter antagonists to the preparation while recording from dually innervated RA neurons. Two dually innervated RA neurons were treated with kynurenic acid (1 mM bath application or 10 mM from a puffer pipette), a broad-spectrum glutamate receptor antagonist (12). Kynurenic acid application was accompanied by a pronounced decrease in the L-MAN and HVC EPSP amplitudes (Fig. 3). The L-MAN EPSP amplitude decreased to 0.30 ± 0.06 and the HVC EPSP amplitude decreased to 0.28 ± 0.06 of their respective control values preceding treatment. Washout of the drug was accompanied by recovery of the HVC EPSP amplitude to 0.98 ± 0.22 of the control value and the L-MAN EPSP amplitude to 1.26 ± 0.02 of the control value. Complete blockade was not achieved with puffer pipette application, probably because the effective bath concentration was too low. Kynurenic acid strongly reduced the L-MAN and HVC EPSPs recorded from dually innervated RA neurons.

The contribution of NMDA receptor-mediated transmission in the L-MAN and HVC EPSPs was tested with the

NMDA receptor antagonist D-APV (13) in 15 dually innervated RA neurons. Two of these cells were examined in normal ACSF, 12 were examined in high divalent ACSF, and 1 was examined in very high divalent ACSF supplemented with $10 \mu\text{M}$ bicuculline methiodide. High divalent ion concentrations were used to suppress polysynaptic transmission. Regardless of the conditions, D-APV ($100 \mu\text{M}$ applied from a puffer pipette) significantly reduced the L-MAN EPSP amplitude, without exerting a significant effect on the HVC EPSP amplitude (see Fig. 4). D-APV reduced the L-MAN EPSP amplitude to 0.43 ± 0.03 of the control value ($P < 0.0001$, $n = 15$). In these same RA neurons, the HVC EPSP amplitude measured in D-APV was 0.98 ± 0.06 of the control value ($P < 0.81$, $n = 15$). In 13 cells where a successful washout of the D-APV was obtained, the L-MAN EPSP amplitude recovered to the control value (1.08 ± 0.08 of the control EPSP amplitude, $P < 0.322$, $n = 13$). The HVC EPSP exhibited an unusual washout effect, occasionally "recovering" to an amplitude greater than either the control or APV values (1.31 ± 0.10 ; $P < 0.005$ with respect to the control conditions, $P < 0.01$ with respect to the APV conditions; $n = 13$). Since the same "excess" recovery of the HVC EPSP also occurred in the presence of $10 \mu\text{M}$ bicuculline methiodide, it is unlikely that this effect can be explained by the presence of a D-APV-sensitive, subtype γ -aminobutyric acid-mediated inhibitory pathway.

In addition to depressing the L-MAN EPSP amplitude, D-APV also reduced the rise time of the L-MAN EPSP. The time to peak of the L-MAN EPSP decreased from 12.28 ± 0.89 msec ($n = 25$) to 6.79 ± 0.87 msec ($n = 15$) in the presence of D-APV ($P < 0.0002$). Although D-APV appeared to reduce the onset slope of the L-MAN EPSP as well, from 1.06 ± 0.12 mV/msec ($n = 25$) to 0.67 ± 0.11 mV/msec ($n = 15$), this effect was not significant ($P < 0.06$). D-APV did not significantly reduce either of these aspects of the HVC EPSP. Note that the time to peak of the L-MAN EPSP measured in the presence of D-APV approximated the control values obtained for the HVC EPSP. Blocking NMDA receptor-mediated components of the L-MAN EPSP unmasked a faster component with a time course similar to the D-APV-resistant HVC EPSP.

Although the HVC EPSP was not reduced by D-APV, it was strongly blocked by the non-NMDA glutamate receptor antagonist CNQX (14). Eight dually innervated RA neurons were treated with CNQX applied from a puffer pipette. Five cells were tested in high divalent ACSF, two were tested in very high divalent ACSF, and one was tested in very high divalent ACSF with $10 \mu\text{M}$ bicuculline methiodide. Regard-

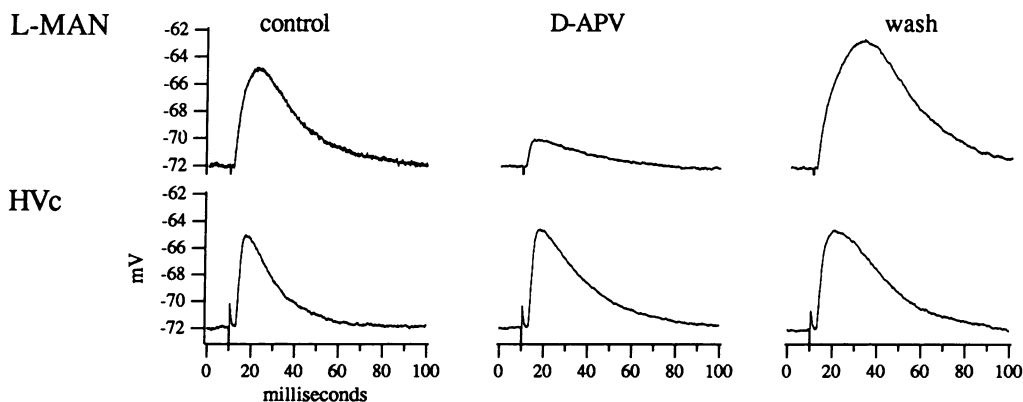


FIG. 4. D-APV ($100 \mu\text{M}$ applied from a puffer pipette) lowered the L-MAN EPSP amplitude, without affecting the amplitude of the HVC EPSP, in dually innervated RA neurons. Fifteen minutes after drug application was discontinued, the L-MAN EPSP had recovered completely (*wash*). Recordings were made in high divalent ACSF; the brain slice was prepared from a 50-day-old male finch. Slight dc hyperpolarization was used to suppress spontaneous firing of action potentials in this example. In all instances, the L-MAN or HVC fiber tracts were stimulated at $t = 10$ msec.

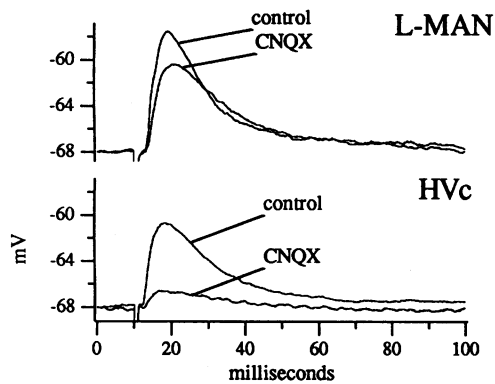


Fig. 5. CNQX (10 μ M applied from a puffer pipette) did not significantly affect the L-MAN EPSP but almost completely abolished the HVC EPSP. This dually innervated RA neuron was impaled in a brain slice made from a 45-day-old male finch, in high divalent ACSF. The cell is shown at its actual resting potential; L-MAN or HVC fiber tracts were stimulated at $t = 10$ msec.

less of the ionic conditions, CNQX always strongly blocked the HVC EPSP (0.27 ± 0.03 of the control value; $P < 0.0001$, $n = 8$), without significantly affecting the L-MAN EPSP (0.93 ± 0.11 of the control value; $P < 0.55$, $n = 8$) (see Fig. 5). A partial or complete washout was accomplished in six of the eight cells treated with CNQX, with the HVC EPSP amplitude recovering to 0.72 ± 0.09 of the control value. The washout amplitude was significantly greater than the amplitude in CNQX ($P < 0.0002$, $n = 6$) but was still lower than the control value ($P < 0.003$, $n = 6$).

The onset slope of the HVC EPSP was also significantly reduced by CNQX treatment, declining from 1.57 ± 0.14 mV/msec ($n = 25$) to 0.44 ± 0.04 mV/msec ($n = 8$) in the presence of CNQX ($P < 0.0001$). The time to peak amplitude increased slightly, from 7.12 msec to 8.76 msec, but this difference was not significant. The onset slope and time to peak of the L-MAN EPSP were not significantly affected by CNQX.

DISCUSSION

Electrical stimulation of the L-MAN and HVC fiber tracts produced EPSPs in the majority of RA neurons from which we recorded. This result suggests that L-MAN and HVC axons form excitatory synapses on many of the same RA neurons. The linear summation of L-MAN and HVC EPSPs supplies evidence that the two stimulating electrodes activated different synapses on the same neuron. Assuming a passive dendritic membrane, the linear summation of these two EPSPs further implies that L-MAN and HVC synapses might be electrically isolated from each other (15). In the canary, serial electron microscopic reconstructions have shown that L-MAN and HVC axons terminate on spinous type IV RA neurons, and these two different synaptic populations are randomly intermixed along the dendrite (16). If the same is true for the RA neurons we recorded from *in vitro*, then the linear interaction of the L-MAN and HVC EPSPs could reflect a more subtle compartmentalization of the dendrite or more complex processes involving an active dendritic membrane.

Although L-MAN and HVC terminals evoke EPSPs from the same RA neurons, these EPSPs appear to be mediated by different glutamate receptor subtypes. D-APV, a specific antagonist of the NMDA subtype of glutamate receptor (13), blocked much of the L-MAN EPSP, even though the HVC EPSP recorded from the same cell was largely unaffected. Treatment with CNQX, an antagonist acting at the quisqualate and kainate subtypes of glutamate receptors (14), strongly blocked the HVC EPSP but exerted no consistent effect on the L-MAN EPSP. Despite the differential effects

of D-APV and CNQX on these two types of EPSPs, however, the broad spectrum glutamate receptor antagonist kynurenic acid (12) blocked both inputs to the same extent. Electrical stimulation of HVC and L-MAN axons thus evokes glutamatergic EPSPs within RA, but these EPSPs are mediated primarily by different subtypes of glutamate receptors.

Several neural circuits use NMDA receptor activation to generate patterned, rhythmic discharge (1, 17, 18). In the lamprey spinal cord, application of NMDA induces oscillatory activity in neurons responsible for generating the rhythmic motor output necessary for swimming (19). EPSPs with NMDA and non-NMDA components can be recorded from the motoneurons and excitatory interneurons (premotor neurons) in this spinal swimming circuit (20). The differential activation of these NMDA and non-NMDA receptors can modulate the output frequency of the circuit (1).

An analogous mechanism may operate to modulate electric organ discharge in certain weakly electric fish. The electric organ discharge (EOD) pattern is under the control of a medullary pacemaker nucleus (PN) (21). The discharge patterns of neurons within the PN, and hence the EOD, can be modulated in two ways by afferents originating in the diencephalic prepacemaker nucleus: in a smooth and graded fashion (i.e., the jamming avoidance response, or JAR) and in an abrupt increase in the discharge rate ("chirps") (2, 3). Pharmacological analyses suggest that the prepacemaker nucleus generates the JAR by activating NMDA receptors within the pacemaker but mediates chirps by exciting non-NMDA receptors in the same region (2, 3). Again, the activation of distinct glutamate receptor subtypes within the same, simple pattern generating circuit can produce strikingly different behaviors.

Many HVC and RA neurons fire bursts of spikes in the same temporal pattern as, but immediately preceding, the bird's actual song vocalization (6). Young birds establish their song's temporal patterns by hearing themselves sing (22, 23). RA neurons are positioned to receive premotor commands from HVC and, presumably, song-related auditory information from L-MAN (11). Our *in vitro* recordings from RA neurons suggest that L-MAN and HVC axons differentially activate NMDA and non-NMDA receptors during a period when vocal plasticity is still quite pronounced. Activation of these two subtypes of glutamate receptors might be used to modulate the output patterns of RA neurons, thus providing a neural mechanism for generating complex and temporally varying vocalizations.

We thank Dr. Gilles Laurent for reading the manuscript. This work was supported by a grant from the McKnight Foundation.

1. Brodin, L., Grillner, S. & Rovainen, C. M. (1985) *Brain Res.* **325**, 302–306.
2. Dye, J., Heiligenberg, W., Keller, C. H. & Kawasaki, M. (1989) *Proc. Natl. Acad. Sci. USA* **86**, 8993–8997.
3. Kawasaki, M. & Heiligenberg, W. (1990) *J. Neurosci.* **10**, 3896–3904.
4. Nottebohm, F., Stokes, T. M. & Leonard, C. M. (1976) *J. Comp. Neurol.* **165**, 457–486.
5. Gurney, M. E. (1981) *J. Neurosci.* **1**, 658–673.
6. McCasland, J. S. (1987) *J. Neurosci.* **7**, 23–39.
7. Okuhata, S. & Saito, N. (1987) *Brain Res. Bull.* **18**, 35–44.
8. Bottjer, S. W., Halsema, K. A., Brown, S. A. & Miesner, E. A. (1989) *J. Comp. Neurol.* **279**, 312–326.
9. Bottjer, S. W., Miesner, E. A. & Arnold, A. P. (1984) *Science* **224**, 901–903.
10. Sohrabji, F., Nordeen, E. J. & Nordeen, K. W. (1990) *Behav. Neural Biol.* **53**, 51–63.
11. Mooney, R. & Doupe, A. J. (1991) *Discuss. Neurosci.* **7**, in press.
12. Perkins, M. N. & Stone, T. W. (1982) *Brain Res.* **247**, 184–187.
13. Davies, J., Francis, A. A., Jones, A. W. & Watkins, J. C. (1981) *Neurosci. Lett.* **21**, 77–81.
14. Honore, T., Davies, S. N., Drejer, J., Fletcher, E., Jacobsen, P., Lodge, D. & Nielsen, F. E. (1988) *Science* **241**, 701–703.

15. Rall, W., Burke, R. E., Smith, T. G., Nelson, P. G. & Frank, K. (1967) *J. Neurophysiol.* **30**, 1169–1193.
16. Canady, R. A., Burd, G. D., DeVogd, T. J. & Nottebohm, F. (1988) *J. Neurosci.* **8**, 3770–3784.
17. Brodin, L. & Grillner, S. (1985) *Brain Res.* **360**, 139–148.
18. Dale, N. & Roberts, A. (1984) *J. Physiol. (London)* **348**, 527–543.
19. Wallen, P. & Grillner, S. (1987) *J. Neurosci.* **7**, 2745–2755.
20. Dale, N. & Roberts, A. (1985) *J. Physiol. (London)* **363**, 35–59.
21. Dye, J. C. & Meyer, J. H. (1986) in *Electroreception*, eds. Bullock, T. H. & Heiligenberg, W. (Wiley, New York), pp. 71–102.
22. Konishi, M. (1965) *Z. Tierpsychol.* **22**, 770–783.
23. Price, P. H. (1979) *J. Comp. Physiol. Psychol.* **93**, 260–277.